Ecological Modelling 233 (2012) 41–51

Contents lists available at SciVerse ScienceDirect

Ecological Modelling

journal homepage: www.elsevier.com/locate/ecolmodel

Analytical approximation of a stochastic, spatial simulation model of fire and forest landscape dynamics

Alan J. Tepley[a,*], Enrique A. Thomann[b]

[a] Departments of Geosciences and Forest Ecosystems and Society, Oregon State University, Corvallis, OR 97331-5506, USA
[b] Department of Mathematics, Oregon State University, Corvallis, OR 97331-4605, USA

ARTICLE INFO

Article history:
Received 13 August 2011
Received in revised form 2 March 2012
Accepted 3 March 2012

Keywords:
Simulation model
Analytical model
Hazard rate
Forest landscape simulation model
Landscape fire succession model

ABSTRACT

Recent increases in computation power have prompted enormous growth in the use of simulation models in ecological research. These models are valued for their ability to account for much of the ecological complexity found in field studies, but this ability usually comes at the cost of losing transparency into how the models work. In order to foster greater understanding of the functioning of computer simulation models, we develop an analytical approximation of the Landscape Age-class Demographics Simulator (LADS; Wimberly, 2002), a representative example of broad group of models that simulate landscape-scale forest dynamics in response to a series of recurring disturbances that interact spatially with existing landscape structure. Much of the model output was produced mathematically, without generating a series of disturbances (in this case, fire) or simulating the forest response to each disturbance. The approximation provides a detailed understanding of the modeled fire regime. Also, it provides equations that directly specify the roles of key input parameters rather than having to infer these roles indirectly from model output in a sensitivity analysis. The application of analytical methods typically has been limited to simple scenarios that lack feedbacks or spatial interactions, but in this exercise, analytical methods address much of the complexity more commonly addressed by simulation: the modeled landscape is composed of two provinces, each with a unique fire frequency and fire-size distribution; stochastic variation in the number of fires per year and the size of each fire; and two levels of fire severity that each have different effects on forest structure. Analytical approximation is not suggested as an alternative to simulation models, but rather, as a complementary approach aimed at improving insight into model function.

1. Introduction

1.1. Background and objectives

Recent increases in computation power have prompted tremendous growth in the use of simulation models to expand upon the insight gained from ecological field studies for understanding longer-term and broader-scale landscape dynamics. For example, landscape-scale forest simulation models have become important tools for broad-scale, strategic management planning in forest landscapes (Keane et al., 2004; Scheller and Mladenoff, 2007; He, 2008). By generating statistical distributions of key variables, such as the abundance and patch-size distributions of old-growth and early-seral forest, these models have made a great contribution to understanding landscape dynamics under historical disturbance regimes and those likely to arise in response to prospective future disturbance or management scenarios.

Although simulation models are valued for their ability to represent the complex feedbacks and spatial interactions characteristic of ecological systems, this ability typically comes at the cost of requiring numerous input parameters and losing transparency into how the models work (Oreskes, 2003). Important problems likely to arise from the lack of tractability typically associated with increasing model complexity include (1) the potential for uncertainty in parameter estimates to propagate in unpredictable ways (DeAngelis and Mooij, 2003), (2) a mismatch between the level of complexity in model algorithms and that needed to address the question of interest, and (3) little understanding of the uncertainty in model output by the audience of ecologists, managers, and policy-makers interested in applying the insight gained from modeling studies (Pielke, 2003).

The objective of this study is to develop an approach for increasing transparency into the function of computer simulation models in general, and specifically, for landscape-scale models of forest dynamics in relation to broad-scale disturbances. To address this

* Corresponding author. Present address: Department of Geography, University of Colorado, 110 Guggenheim Hall, Campus Box 260, Boulder, CO 80309-0260, USA. Tel.: +1 303 492 4785; fax: +1 303 492 7501.
E-mail addresses: Alan.Tepley@Colorado.edu, tepleya@geo.oregonstate.edu (A.J. Tepley), thomann@math.orst.edu (E.A. Thomann).

0304-3800/$ – see front matter © 2012 Elsevier B.V. All rights reserved.
doi:10.1016/j.ecolmodel.2012.03.005

objective, we develop an analytical approximation of the Landscape Age-class Demographics Simulator (LADS, version 2.2; Wimberly, 2002). The approximation translates the model algorithms into a tractable form (i.e., one that can be solved mathematically without generating a series of recurring fires or the response of vegetation to each fire), and by doing so, it directly specifies the roles of key input parameters and the interactions among them.

LADS is a member of a broad group of models labeled as Landscape Fire Succession Models (Keane et al., 2004) or Forest Landscape Simulation Models (Scheller and Mladenoff, 2007; He, 2008). These models simulate the response of forest vegetation at the stand level to at least one recurring, landscape-scale disturbance, with stochasticity in the initiation, spread, extent, and severity of each disturbance event. The models are implemented over an area broad enough (1000s to 100,000s of km^2) and a time period long enough (centuries to millennia) to generate statistical distributions of the abundance and patch sizes of forests with different attributes (e.g., age classes or stand structures). Space and time are represented explicitly, by deriving forest attributes at each stand from those in the previous timestep and allowing the disturbances to spread among stands depending on landscape configuration (He, 2008).

LADS was selected because its approaches for modeling fire spread and forest succession are similar to those applied in other landscape-scale forest simulation models, and its complexity for these processes is intermediate among models. LADS models forest succession using a state-and-transition approach, where stands proceed along a pre-defined series of structural stages in the absence of disturbance. Following fire, the series either is reset, or stands shift to an alternate pathway, depending on fire severity (Wimberly, 2002). The ease of developing, parameterizing, and initializing state-and-transition models favors widespread use of this approach in other models (Kurz et al., 2000; Keane et al., 2002, 2004). Simpler models have a single pathway reset only by high-severity fire (Boychuk et al., 1997), whereas more complex models track changes in community composition over time at the level of individual trees, tree species, or plant functional types (He et al., 2005; Keane et al., 2011). LADS models fire spread using a cellular-automata approach designed to generate burned patches that resemble historical fires in size and shape while limiting the mechanistic detail in the fire-spread process in order to facilitate computational efficiency in generating numerous fires (Wimberly, 2002).

This study evaluates version 2.2 of LADS, which initially was applied to estimate the historical variability in the abundance of old-growth forests in the Oregon Coast Range (Wimberly, 2002; Nonaka and Spies, 2005). The estimated variability then served as a baseline for evaluating present landscape conditions and those likely to develop under alternate management scenarios (Nonaka and Spies, 2005; Thompson et al., 2006). A detailed description of LADS is provided by Wimberly (2002). A brief overview of the model is provided below (Section 1.2), followed by an explanation of the theory for relating fire-frequency information to the stand-age distribution of a forest landscape (Section 2) and our application of this theory to produce an analytical approximation of the simulation model (Section 3). Then the accuracy of the approximation and its usefulness for understanding the role of input parameters are evaluated by comparing results of the calculations to the output of the simulation model (Section 4). Finally, the new insights and limitations of the analytical approach are discussed (Section 5) along with the value of combining modeling approaches (Section 6).

1.2. Simulation model

In previous applications of LADS to the Oregon Coast Range, the landscape was divided into Coastal and Valley Margin provinces to account for a trend of increasing fire frequency, smaller fires, and lower fire severity with decreasing precipitation from the coast to the margin of the Willamette Valley (Wimberly, 2002). The natural fire rotation (NFR) of the Coastal Province (200 years) was set at twice that of the Valley Margin (100 years; Table 1) based on tree ring and lake sediment studies (Impara, 1997; Long et al., 1998). The fire-size distribution of each province was derived from historical vegetation maps (Teensma et al., 1991).

The number of fires per timestep and the size of each fire are determined using random variables (Fig. 1), which allows the area burned per timestep to fluctuate around a fixed mean (Wimberly, 2002). Fires are simulated by first determining the average number of fires per timestep in each province (λ_j; Table 1), which is done by dividing province area by the product of its NFR and its mean fire size (Boychuk et al., 1997). This average serves as the parameter for a Poisson random variable used to simulate the number of fires per timestep (Fig. 1).

Each fire is initiated in a random cell and spreads stochastically until burning an area determined at the time of ignition (Fig. 1). The probability of ignition is weighted to make ignitions most likely on upper slopes and in the most flammable age classes. Susceptibility to fire ignition and spread from adjacent cells follows a U-shaped function of stand age, with the greatest susceptibility in young stands assumed to retain dead wood from the previous stand and in old-growths stands that have abundant fuel in all size classes (Agee and Huff, 1987). At the time of each ignition, fire size is drawn from a lognormal distribution (Fig. 1) with a unique mean and standard deviation (SD) of fire size in each province (Wimberly, 2002; Table 1).

The fire-spread algorithm is a cellular-automata-based subroutine designed to allow fire to spread most readily along upper slopes and in the most susceptible age classes (Wimberly, 2002; Fig. 1). User-defined parameters for windspeed and wind direction also influence fire spread. Susceptibility to fire spread is calculated as the product of susceptibility scores based on stand age, topographic position, and wind variables (Wimberly, 2002). For each of the eight cells adjacent to a burning cell, a uniform random variable is drawn on the interval (0, 1), and the cell burns if its susceptibility exceeds this value (Wimberly et al., 2000). The algorithm repeats until the area burned reaches the fire size drawn at the time of ignition (Fig. 1).

Each fire produces a mosaic of low- and high-severity patches where the proportion of cells that burn at high severity increases with fire size (Wimberly, 2002). To enable greater representation of high burn severity in larger fires, fire size is divided into three classes: small (<100 km^2), medium (100–500 km^2), and large (>500 km^2) (Table 1). For each burned cell, a uniform random variable is drawn on the interval (0.0, 0.5) for small fires, (0.1, 0.8) for medium fires, and (0.7, 0.95) for large fires. The cell burns at high severity if a second uniform random variable on the interval (0, 1) is smaller than the first (Fig. 1).

Each cell has two state variables—the time since the last high-severity fire (AGE) and the time since the most recent fire, regardless of severity (TFIRE)—which allow for two pathways of forest structural development (Wimberly, 2002; Fig. 1). In one pathway, high-severity fire converts stands to an open condition, from which single-story stands develop in the absence of fire. In the other pathway, low-severity fire converts stands to a semi-open condition that develops into multi-story stands (Wimberly, 2002). Semi-open stands are defined as those that have not burned at high severity for at least 30 years and have experienced at least one low-severity fire in the last 30 years (AGE > 30 and TFIRE $\leq$ 30). Multi-story stands have not burned at high severity for at least 80 years and have experienced at least one low-severity fire in the last 80 years, but not within the last 30 years (AGE > 80 and 30 < TFIRE $\leq$ 80) (Wimberly, 2002).

Table 1
Input parameters for LADS, as parameterized for the Oregon Coast Range (Wimberly, 2002). To facilitate comparison to equations used in the analytical approximation, values for the average number of fires per timestep (λ_j) was calculated assuming a one-year timestep. This value may be multiplied by 10 for a 10-year timestep, as used in LADS.

Variable	Notation/Equation[a]	Coastal Province	Valley Margin
Area of the jth province (km^2)	A_j	14,540	8880
Natural fire rotation (years)	NFR_j	200	100
Mean fire size (km^2)	MFS_j	73	22.5
SD of fire size (km^2)	$SDFS_j$	320.5	50
Parameters for the lognormal fire-size distribution	$\mu_j = \ln[MFS_j^2/\sqrt{(MFS_j^2 + SDFS_j^2)}]$	2.786	2.223
	$\sigma_j = \sqrt{\ln[1 + (SDFS_j^2/MFS_j^2)]}$	1.735	1.335
Average number of fires initiated in the jth province (#/year); used as the parameter for the Poisson random variable that determines the number of fires per timestep	$\lambda_j = A_j/(NFR_j \times MFS_j)$	0.996	3.947
Minimum (Min_k) and maximum (Max_k) size (km^2) for fires in the kth size class (k = 1, 2, or 3, for small, medium, and large fires, respectively)	(Min_1, Max_1) (Min_2, Max_2) (Min_3, Max_3)	(0, 100) (100, 500) (500, ∞)	(0, 100) (100, 500) (500, ∞)
Lower (l_k) and upper (u_k) bounds for the random variable (U_k) used to determine the probability of burning at high severity for a fire in the kth size class	(l_1, u_1) (l_2, u_2) (l_3, u_3)	(0, 0.5) (0.1, 0.8) (0.7, 0.95)	(0, 0.5) (0.1, 0.8) (0.7, 0.95)

[a] In all formulas, the subscripts j and k refer to a particular province or fire-size class, respectively.

Simulations are conducted on a grid of 9-ha cells (Nonaka and Spies, 2005) with a buffer around the Coast Range that allows fires to spread into and out of the analysis area (Wimberly, 2002). Replications are initiated by conducting a burn-in period in which simulations are run without recording output in order to overwrite the initial stand ages (Fig. 1).

2. Theory

A fundamental characteristic of models that simulate the effects of recurring disturbances (in this case, fire) on the abundance of different forest conditions (e.g., age classes or stand structures) across a landscape is the rate of burning at each level of severity. Understanding how the model simulates these rates of burning is key to approximating the model analytically. The rate of burning, referred to as the hazard of burning, or hazard rate, is the age-specific probability rate of fire (Johnson and Gutsell, 1994). It is not strictly a probability (values are not constrained between 0 and 1), but rather, a probability rate. However, on an annual timestep, viewing the hazard rate as the annual probability of fire for stands of a given age provides an estimate almost identical to the probability of fire in that year (Reed, 1994). The hazard rate should not be confused with fire hazard, as used in fire ecology as a measure of potential fire behavior based on fuel loading.

The use of the hazard rate to determine a probability density function for stand age previously was described by Johnson and Gutsell (1994). An overview of this approach is provided below to introduce the notation used in subsequent equations and to illustrate the derivation of several useful functions from the hazard rate.

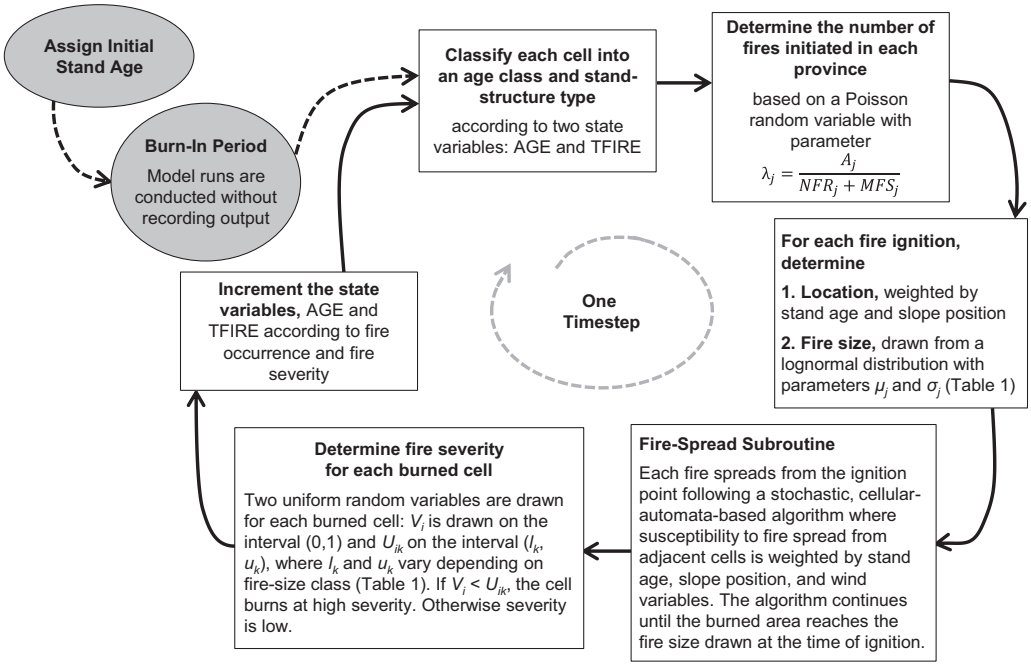

Fig. 1. Flow chart of the major processes conducted in the simulation model, LADS (version 2.2; Wimberly, 2002). Gray ovals represent the steps involved in model initiation, prior to recording output. White boxes represent the series of processes conducted in each timestep. Variables given in the boxes are defined in Table 1 and in the text.

In the following equations, τ is a random variable representing the number of years between successive fires that burn a given cell at high severity (regardless of the number of times it burned at low severity in the intervening period). In all equations, t represents stand age, which is reset only by high-severity fire, and thus is equivalent to the state variable, AGE, in LADS.

The hazard rate for high-severity fire, $h_\tau(t)$, is the probability that a cell burns at high severity on the interval $(t, t+\Delta t)$, provided it has reached age t without high-severity fire:

$$h_\tau(t) = \lim_{\Delta t \to 0} [P\{\tau \in (t, t+\Delta t) | \tau > t\}] \frac{1}{\Delta t}.$$

The cumulative survivorship distribution, $S_\tau(t)$, is the probability of a cell reaching age t without high-severity fire:

$$S_\tau(t) = \exp\left[-\int_0^t h_\tau(u)du\right]. \quad (1)$$

In Eq. (1) and in the following equations, u is a dummy variable used to clarify that $S_\tau(t)$ is a function of the upper level of integration, t, and not a function of u. The probability density function for the intervals between high-severity fires, $f_\tau(t)$ (i.e., the density function for intervals between successive fires that burn a given cell at high severity, regardless of the number of times if burns at low severity in the intervening period), is the probability of a cell reaching age t without high-severity fire, $S_\tau(t)$, multiplied by the probability of experiencing high-severity fire in the next timestep, $f_\tau(t)$:

$$f_\tau(t)\Delta t = P\{\tau \in [t, t+\Delta t]\} = S_\tau(t)h_\tau(t)\Delta t$$
$$= h_\tau(t)\exp(-\int_0^t h_\tau(u)du)\Delta t. \quad (2)$$

The above functions are related by $h_\tau(t) = f_\tau(t)/S_\tau(t)$.

For a given cell, the mean interval between successive high-severity fires, $E(\tau)$, is determined by integrating the survivorship distribution over all stand ages:

$$E(\tau) = \int_0^\infty S_\tau(t)dt = \int_0^\infty \exp\left[-\int_0^t h_\tau(u)du\right] dt. \quad (3)$$

If the hazard of burning at high severity follows the same function of stand age in all cells, $E(\tau)$ represents the NFR for high-severity fire, or the average number of years for a cumulative area equal to the extent of the landscape to be burned at high severity (Heinselman, 1973).

The hazard rate for high-severity fire may be used to determine the probability density function for stand age under the following assumptions: (1) trees establish promptly after fire and tree longevity exceeds intervals between high-severity fires, such that stand age is equivalent to the time since the last high-severity fire; (2) only high-severity fire kills the existing forest and initiates a new stand; and (3) the landscape has undergone several fire rotations without changes in the hazard rate for high-severity fire. The first two assumptions are equivalent to defining the state variable, AGE, as the number of years since the last high-severity fire and excluding non-fire disturbances in LADS. The third assumption is analogous to the use of a burn-in period prior to recording model output and holding all input parameters values constant over the analysis period (Wimberly, 2002; Nonaka and Spies, 2005).

To calculate the probability density function for stand age, it is useful to recognize that the reciprocal of the mean interval between high-severity fires at each cell, $1/E(\tau)$, represents the proportion of the landscape expected to burn at high severity each year. Because landscape size is fixed, and by assumptions 1 and 2, a new stand initiates only after another stand is killed by high-severity fire, $1/E(\tau)$ also represents the frequency of stand establishment, or the average proportion of the landscape covered by new stands initiated each year. The probability density function for stand age, $a_\infty(t)$, is calculated by multiplying the frequency of stand establishment, $1/E(\tau)$, by the probability of stands reaching age t without high-severity fire, $S_\tau(t)$:

$$a_\infty(t) = \frac{1}{E(\tau)} S_\tau(t) = \frac{1}{\int_0^\infty \exp\left[-\int_0^t h_\tau(u)du\right] dt} \exp\left[-\int_0^t h_\tau(u)du\right]. \quad (4)$$

Eq. (4) specifies the probability that the age of a random cell is equal to t in a given year provided assumptions 1–3, above. Also, by assumption 3, $a_\infty(t)$ is an equilibrium density function in the sense that it does not depend on the year in which it is calculated.

If the hazard rate for high-severity fire follows the same function of stand age in all cells, $a_\infty(t)$ provides the proportion of the landscape expected to support stands of each age. However, the proportion of the landscape observed to support stands of each age in any year will diverge from the density function except in the unlikely scenario where landscape size is so large relative to the variation in the number of ignitions per year and fire size that there is no variation in annual area burned (Turner and Romme, 1994; Wimberly et al., 2000). Nevertheless, if all input parameters are fixed and the abundance of each age class is averaged over time within a model run or across replications, the abundance of each age class averaged over time or across replications eventually will converge to $a_\infty(t)$.

3. Calculation

3.1. Derivation of hazard rates

The first step in approximating the proportion of the Oregon Coast Range expected to support stands of each age, as simulated by LADS, is to determine the rate at which stands burn at low and high severity (i.e., the hazard rates for low- and high-severity fire) (Fig. 2). In doing so, we have to make the simplification of excluding influences of stand age and topographic position on susceptibility to fire ignition and spread. Eqs. (1)–(4) apply whether or not stand age (i.e., fuel loading or microclimatic variation as a function of time since fire) feeds back on the annual probability of fire occurrence (McCarthy et al., 2001). However, in LADS, these influences are incorporated into the fire-spread algorithm (Wimberly, 2002), which means the proportion of cells in each age class and topographic position burned by a given fire depends on the location of the ignition and the pattern of different age classes at the time of the fire. Therefore, the difference between the expected age distribution determined analytically without accounting for influences of stand age and topographic position and the average simulated abundance of each age class provides a measure of the strength of these influences.

The overall hazard rate (regardless of fire severity) is represented by $h^{(j)}(t)$, where the index, j, indicates there is a unique function for each province. The overall hazard rate in each province can be determined by multiplying the average number of fires per year in the province, λ_j (Table 1), by the probability that a random cell in that province is burned by each fire:

$$h^{(j)}(t) = \lambda_j \times P\{b_i = 1\}, \quad (5)$$

where b_i has a value of 1 if the ith cell is burned by a given fire, and 0 otherwise.

When the hazard rate is independent of stand age, the probability that a random cell is burned by a single fire of known size can be determined by conditioning on the size of the fire: $P\{b_i = 1 | X = x\} = x/A_j$ (Boychuk et al., 1997), where X represents fire size, and A_j represents the area of the jth province (Table 1). For

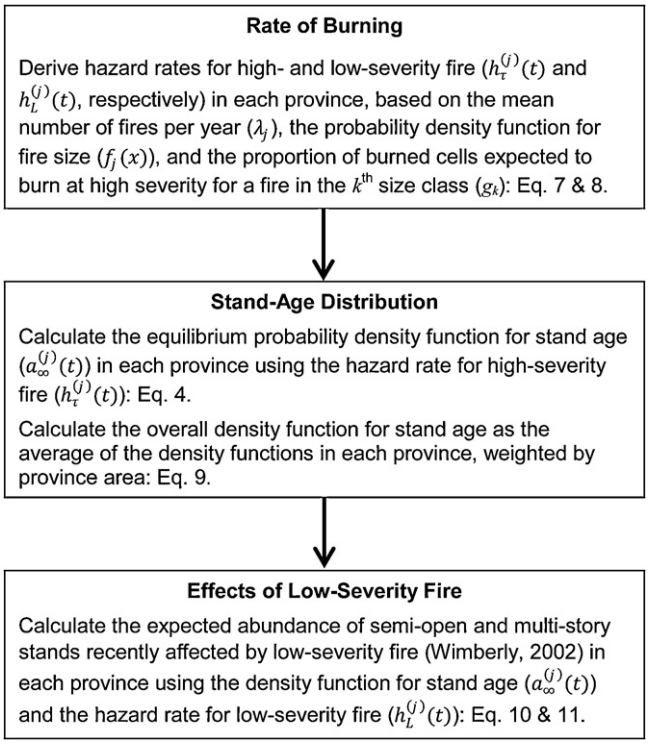

Fig. 2. The steps involved toward approximating the expected abundance of stands in each age class and of two stand-structure types recently affected by low-severity fire, as determined by the stochastic, spatial simulation model, LADS (version 2.2; Wimberly, 2002).

a series of recurring fires, where fire size is drawn from a known density function, $f_j(x)$, conditioning on fire size enables calculation of the probability that a given cell is burned per ignition without simulating the size of each fire:

$$P\{b_i = 1\} = \int_0^\infty P\{b_i = 1 \,|\, X\} f_j(x)dx = \int_0^\infty \frac{x}{A_j} f_j(x)dx. \quad (6)$$

Therefore, Eq. (5) can be solved as

$$h^{(j)}(t) = \lambda_j \times P\{b_i = 1\} = \lambda_j \times \int_0^\infty \frac{x}{A_j} f_j(x)dx = \lambda_j \times \frac{MFS_j}{A_j} = \frac{1}{NFR_j},$$

where MFS_j and NFR_j, are the user-defined mean fire size and natural fire rotation, respectively, of the jth province (Table 1). Thus, when the annual probability of fire occurrence is independent of stand age or location, the hazard rate is simply the reciprocal of the NFR, even with contagious fire spread and stochastic variation in annual area burned around a fixed mean.

To determine the hazard rate for high-severity fire, $h_\tau^{(j)}(t)$, the average number of fires per year in each province, λ_j, is multiplied by the joint probability that a random cell is burned by each fire and it burns at high severity:

$$h_\tau^{(j)}(t) = \lambda_j \times P\{b_i = 1, \omega = 1\}, \quad (7)$$

where ω_i has a value of 1 if the ith cell is burned at high severity and 0 otherwise.

In LADS, fire severity is determined based on a uniform random variable, U_{ik}, drawn cell-by-cell on a different interval for each fire-size class (Table 1). Values of U_{ik} are compared to a second uniform random variable, V_i, drawn on the interval (0, 1) for each cell. The ith cell burns at high severity if $V_i < U_{ik}$ (Fig. 1). Therefore, given that the ith cell is burned by a fire in the kth size class, the probability that it burns at high severity is provided by:

$$p\{\omega_i = 1\} = P\{V_i < U_{ik}\} = E(U_{ik}).$$

Because U_{ik} and V_i are drawn independently for each cell, the proportion of the cells burned by fires in the kth size class expected to experience high-severity fire, g_k, is provided by the expected value of the uniform random variable, U_{ik}.

The joint probability that a random cell is burned ($b_i = 1$) and fire severity is high ($\omega_i = 1$) is determined by multiplying the probability that the ith cell is burned by a fire in each size class by the proportion of cells burned by a fire of that class expected to experience high-severity fire, and then summing across $m = 3$ classes:

$$P\{b_i = 1, \omega_i = 1\} = \sum_{k=1}^{m} \left(g_k \int_{Min_k}^{Max_k} \frac{x}{A_j} f_j(x)dx \right) = g_1 \int_0^{100} \frac{x}{A_j} f_j(x)dx + g_2 \int_{100}^{500} \frac{x}{A_j} f_j(x)dx + g_3 \int_{500}^{\infty} \frac{x}{A_j} f_j(x)dx. \quad (8)$$

In the above equation, Min_k and Max_k are the user-defined minimum and maximum area burned by fires of the kth size class (Table 1). These values are defined such that $Min_1 = 0$, $Max_k = Min_{k+1}$, and $Max_m = \infty$.

Because fire size is drawn from a lognormal distribution, the density function for fire size, $f_j(x)$, is given by,

$$f_j(x) = \frac{1}{x\sigma_j\sqrt{2\pi}} \exp\left[-\frac{1}{2} \left\{ \frac{(\ln(x) - \mu_j)^2}{\sigma_j^2} \right\} \right],$$

where parameters, μ_j and σ_j, are given in Table 1. Thus, each integral in Eq. (8) can be solved as

$$g_k \int_{Min_k}^{Max_k} \frac{x}{A_j} f_j(x)dx = g_k \left[\frac{1}{A_j} \exp\left(\mu_j + \frac{1}{2}\sigma_j^2 \right) \times (Z_k - Y_k) \right],$$

where

$$Z_k = \Phi\left(\frac{\ln(Max_k) - (\mu_j + \sigma_j^2)}{\sigma_j} \right), \; Y_k = \Phi\left(\frac{\ln(Min_k) - (\mu_j + \sigma_j^2)}{\sigma_j} \right),$$

and $\Phi(x)$ represents the value of the standard normal distribution at x. The values, Z_k and Y_k, represent the proportion of the total area burned over a long simulation that is expected to be burned by fires smaller than the upper and lower bound, respectively, of the kth size class.

Assuming the annual probability of fire occurrence and fire severity are independent of stand age, the hazard rate for low-severity fire is calculated as the difference between the overall hazard of burning and the hazard rate for high-severity fire: $h_L^{(j)}(t) = h^{(j)}(t) - h_\tau^{(j)}(t)$. This relationship is verified by modifying Eqs. (7) and (8) to determine the joint probability that a cell is burned and fire severity is low ($P\{b_i = 1, \omega_i = 0\}$), and replacing g_k with the proportion of cells expected to experience low-severity fire for a fire in the kth size class ($1 - g_k$).

3.2. Stand-age distribution

The probability density function for stand age in each province, $a_\infty^{(j)}(t)$, is determined by Eq. (4) using the hazard rate for high-severity fire (Eqs. (7) and (8)). Then, the expected abundance of each age class across the entire Coast Range is calculated by weighting

the density function for stand age in each province by the proportion of the total landscape represented by that province:

$$a_\infty(t) = \frac{A_1}{\sum_{j=1}^{n} A_j} a_\infty^{(1)}(t) + \cdots + \frac{A_n}{\sum_{j=1}^{n} A_j} a_\infty^{(n)}(t), \quad (9)$$

where n is the number of provinces. Eq. (9) is provided in general form for application to any number of provinces. For the two provinces of the Coast Range, Eq. (9) is reduced to

$$a_\infty(t) = \frac{A_C}{A_C + A_V} a_\infty^{C}(t) + \frac{A_V}{A_C + A_V} a_\infty^{V}(t),$$

where A_C and A_V represent the area, and $a_\infty^C(t)$ and $a_\infty^V(t)$ are the density functions for stand age in the Coastal and Valley Margin provinces, respectively.

3.3. Effects of low-severity fire

The probability density function for stand age, $a_\infty(t)$, is used along with the hazard rate for low-severity fire, $h_L^{(j)}(t)$, to determine the proportion of each province expected to support semi-open and multi-story stand structures recently affected by low-severity fire (Wimberly, 2002; Fig. 2). The probability that a stand has not burned at low severity over a certain range of ages is determined by evaluating the survivorship distribution over the specified age range in a manner analogous to Eq. (1), but replacing the hazard rate for high-severity fire ($h_\tau(t)$) with the hazard rate for low-severity fire ($h_L(t)$). This gives

$$S_L(t) = \exp\left[-\int_0^t h_L(u)du\right].$$

The probability of experiencing at least one low-severity fire over a range of ages is determined by evaluating $1 - S_L(t)$ over the specified age range.

The proportion of each province expected to support stands in the semi-open stand-structure class of Wimberly (2002; AGE > 30 and TFIRE ≤ 30) is calculated by multiplying the expected abundance of stands of each age ($t > 30$), by the probability of experiencing at least one low-severity fire in the previous 30 years, and summing across ages:

$$\text{Proportion semi-open} = \sum_{t=31}^{\infty}\left[a_\infty^{(j)}(t)\left\{1 - \exp\left(-\int_{t-30}^{t} h_L^{(j)}(u)du\right)\right\}\right]. \quad (10)$$

The proportion of each province expected to support multi-story stands (Wimberly, 2002; AGE > 80 and 30 < TFIRE ≤ 80) is determined by finding the proportion of stands of each age ($t > 80$) expected to have experienced at least one low-severity fire in the last 80 years, but not within the last 30 years:

$$\text{Proportion multi-story} = \sum_{t=81}^{\infty}\left[\begin{array}{c} a_\infty^{(j)}(t)\left\{1 - \exp\left(-\int_{t-80}^{t-30} h_L^{(j)}(u)du\right)\right\} \\ \left\{\exp\left(-\int_{t-30}^{t} h_L^{(j)}(u)du\right)\right\} \end{array}\right]. \quad (11)$$

Previous publications using LADS have not reported the average abundance of the semi-open and multi-story stands. Therefore, we conducted a 50,000-year simulation of LADS following a 1000-year burn-in period, using input parameters according to previous studies of the historical range of variability in landscape structure of the Oregon Coast Range (Wimberly, 2002; Nonaka and Spies, 2005). Then, the analytically determined abundance of semi-open and multi-story stands was compared to that averaged over time in the simulation.

4. Results

4.1. Stand-age distribution

After assuming the annual probability of a cell burning is independent of the timing or severity of previous fires and cell location within a province, Eq. (6) illustrates that the overall hazard rate (regardless of severity) is the reciprocal of the user-defined overall NFR for each province: 0.005 and 0.01 for the Coastal and Valley Margin provinces, respectively (Table 2). The above assumption leads to a probability density function for the intervals between successive fires at any cell, $f_\tau(t)$, that is exponential in form (Eq. (2)).

For fires of the kth size class, the proportion of burned cells that is expected to experience high-severity fire is $g_1 = 0.25$, $g_2 = 0.45$, and $g_3 = 0.825$, for small, medium, and large fires, respectively. Thus, by Eq. (8), for each fire initiated in the Coastal Province, the joint probability that a random cell in that province is burned and fire severity is high is 2.77×10^{-3}. For fires initiated in the Valley Margin the joint probability is 8.45×10^{-4} (Table 2). Multiplying the above values by the average number of fires initiated per year in each province (λ_j; Table 1) provides the hazard rate for high-severity fire: $h_\tau^{(C)}(t) = 2.76 \times 10^{-3}$ and $h_\tau^{(V)}(t) = 3.34 \times 10^{-3}$ in the Coastal and Valley Margin provinces, respectively (Eq. (7); Table 2).

The above hazard rates entered into Eqs. (4) and (9) provide an analytically-determined percentage of the Coast Range expected to support each of seven age classes within 1.1% of the abundance of each age class averaged over time within model runs and across replications of the simulation model (Table 3). The analytically-determined expected abundance of all but three classes (Mature, Mid Old Growth, and Late Old Growth) is within 0.5% of their average abundance determined by simulation.

Under the assumption that the annual probability of a cell burning at high severity is independent of the time since the previous fire, the NFR for high-severity fire (362 years in the Coastal Province and 300 years in the Valley Margin) is the reciprocal of the hazard rate for high-severity fire (Eq. (3)). Also, under this assumption, the probability density functions for the intervals between successive high-severity fires (Eq. (2)) and for stand age (Eq. (4)) in each province both are exponential in form.

4.2. Abundance of stand structures

The approximation provides proportions of each province expected to support stands recently affected by low-severity fire that closely match those averaged over a 50,000-year simulation (Table 4). The analytically determined percentages of the Coastal and Valley Margin provinces expected to support semi-open stands (6.0 and 16.4%, respectively) are within 1% of that averaged over the simulation (6.9 and 15.6%, respectively). Likewise, for multi-story stands, the analytically determined expected abundance in the Coastal and Valley Margin provinces (7.9 and 17.8%, respectively) both are within 1.5% of that averaged over the simulation (8.9 and 16.3%, respectively; Table 4).

The hazard rate for low-severity fire ($h_L^{(C)}(t) = 2.24 \times 10^{-3}$ and $h_L^{(V)} = 6.66 \times 10^{-3}$ in the Coastal and Valley Margin provinces, respectively; Table 2) was found by subtracting the hazard rate for high-severity fire from the overall hazard or burning. Under the assumptions that the hazard rate for low-severity fire in a given cell is independent of the time since the most recent fire or its severity, the NFR for low-severity fire (447 years in the Coastal Province and 150 years in the Valley Margin; Table 2) is the reciprocal of this hazard rate (Eq. (3)).

Table 2
Calculations used to approximate the equilibrium age distribution produced by LADS, as parameterized for the Oregon Coast Range in studies of Wimberly (2002) and Nonaka and Spies (2005). Variables not defined below are input parameters defined in Table 1.

Variable	Equation[a]	Coastal Province	Valley Margin
Average proportion of cells that experience high-severity fire for fires in the kth size class	$g_k = (l_k + u_k)/2$	$g_1 = 0.250\, g_2 = 0.450\, g_3 = 0.825$	$g_1 = 0.250\, g_2 = 0.450\, g_3 = 0.825$
For each fire initiated in the jth province, the joint probability that the ith cell is burned ($b_i = 1$) and fire severity is high ($\omega_i = 1$)	$P\{b_i = 1, \quad \omega_i = 1\} = \sum_{k=1}^{m} \left(g_k \int_{Min_k}^{Max_k} \frac{x}{A_j} f_j(x)dx \right)$ m is the number of fire-size classes	2.77×10^{-3}	8.45×10^{-4}
Proportion of total area burned that is expected to be burned by fires smaller than the upper bound of the kth size class[a]	$Z_k = \Phi\left(\frac{\ln(Max_k) - (\mu_j + \sigma_j^2)}{\sigma_j} \right)$	$Z_1 = 0.246\, Z_2 = 0.596\, Z_3 = 1.000$	$Z_1 = 0.674\, Z_2 = 0.951\, Z_3 = 1.000$
Proportion of the total area burned that is expected to be burned by fires smaller than the lower bound of the kth size class[b]	$Y_k = \Phi\left(\frac{\ln(Min_k) - (\mu_j + \sigma_j^2)}{\sigma_j} \right)$	$Y_1 = 0.000\, Y_2 = 0.246\, Y_3 = 0.596$	$Y_1 = 0.000\, Y_2 = 0.674\, Y_3 = 0.951$
Proportion of total area burned expected to be burned by fires in the kth size class	$Q_k = Z_k - Y_k$	$Q_1 = 0.246 Q_2 = 0.349 Q_3 = 0.404$	$Q_1 = 0.674 Q_2 = 0.277 Q_3 = 0.049$
Overall hazard of burning	$h^{(j)}(t) = 1/NFR_j$	0.005	0.010
Hazard rate for high-severity fire	$h_\tau^{(j)}(t) = \lambda_j \times P\left\{ b_i = 1, \quad \omega_i = 1 \right\}$	2.76×10^{-3}	3.34×10^{-3}
Hazard rate for low-severity fire	$h_L^{(j)}(t) = h^{(j)}(t) - h_\tau^{(j)}(t)$	2.24×10^{-3}	6.66×10^{-3}
Natural fire rotation for high-severity fire	$NFR_j^H = 1/h_\tau^{(j)}(t)$	362	300
Natural fire rotation for low-severity fire	$NFR_j^L = 1/h_L^{(j)}(t)$	447	150
Probability density function for stand age of the jth province	$a_\infty^j(t) = h_\tau^{(j)}(t) \times \exp(-\int_0^t h_\tau^{(j)}(u)du)$		
Overall probability function for stand age (n represents the number of provinces)	$a_\infty(t) = \frac{A_1}{\sum_{j=1}^{n} A_j} a_\infty^1(t) + \cdots + \frac{A_n}{\sum_{j=1}^{n} A_j} a_\infty^n(t)$	See Table 3	

[a] In all equations, subscripts, i, j, and k, refer to a given cell, province, or fire-size class, respectively.
[b] $\Phi(x)$ represents the value of the standard normal distribution at x.

4.3. Effects of input parameters

The expected abundance of each age class is highly sensitive to changes in the overall NFR (i.e., the NFR of the province regardless of fire severity) (Fig. 3a) due to a linear relationship between the overall NFR and the NFR for high-severity fire, as explained below. The mean number of fires per year in each province (λ_j) has an inverse linear relationship with the overall NFR of the province, given by $\lambda_j = A_j/(NFR_j \times MFS_j)$ (Table 1). Also, the mean number of fires per year is the only term in the equation for the hazard rate for high-severity fire affected by a change in the overall NFR, and the hazard rate for high-severity fire scales linearly with this value (Eq. (7)). Thus, the NFR for high-severity fire in each province also scales linearly with the overall NFR of the province.

For a given mean and SD of fire size, the slope of the linear relationship between the overall NFR and the NFR for high-severity fire is determined by the proportion of cells expected to burn at high severity for a fire in each size class, g_k (Table 2). The area burned each year, as determined by the number of fires and the size of each fire, is unrelated to g_k. However, changing g_k affects the mean area expected to burn at high and low severity each year. For example, reducing values of g_k by 10% causes the area within the 14,540-km^2 Coastal Province expected to burn at high severity each year to decrease from 4017 ha to 3617 ha, which leads to greater abundance of the oldest age class and lower abundance of the youngest classes (Fig. 3b).

Adjusting each parameter of the fire-size distribution individually by as much as ±50% from its baseline value has little influence on the expected abundance of each age class (Fig. 3c and d). Parameters of the fire-size distribution do not affect the expected area burned per year: when the mean fire size of a province is increased or decreased, the expected number of fires per year in that province adjusts according to the relationship, $\lambda_j = A_j/(NFR_j \times MFS_j)$ (Table 1), to compensate for the larger or smaller fires and thereby maintain the same mean annual area burned. Parameters of the fire-size distribution affect the expected age distribution only through their

Table 3
Comparison of the equilibrium age-class distribution for the Oregon Coast Range produced by LADS to that produced by an analytical approximation using the same fire-regime parameters.

Age class	Age range	Percentage of landscape	
		Simulation[a]	Approximation
Very open	0–10	2.7	2.9
Patchy open	11–20	2.7	2.9
Young	21–80	15.3	15.4
Mature	81–200	23.0	23.6
Early old growth	201–450	28.3	28.8
Mid old growth	451–800	16.2	16.9
Late old growth	>800	10.5	9.4

[a] From Appendix A of Nonaka and Spies (2005). Values were averaged over time within each of 200, 1000-year replications, then these values were averaged across replications.

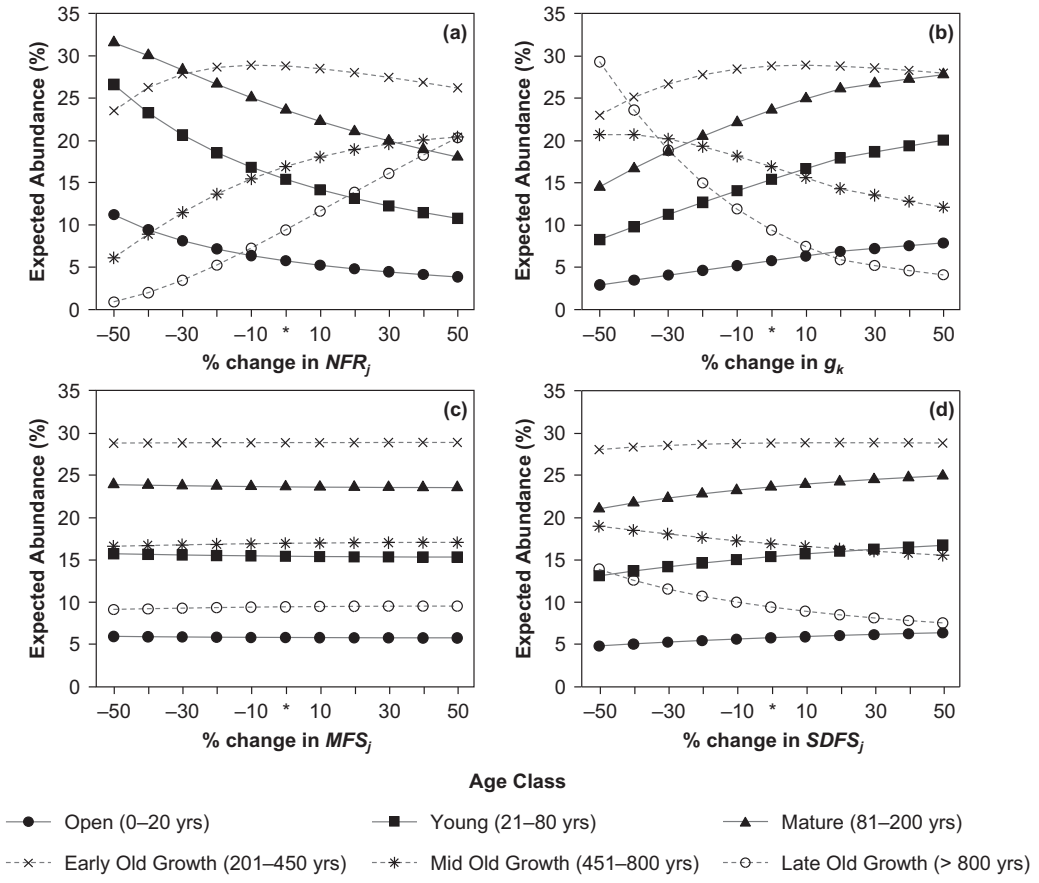

Fig. 3. The proportion of the Oregon Coast Range expected to support stands of six age classes over a range of values of (a) the overall NFR, (b) the proportion of burned cells that burn at high-severity for a fire of the kth size class, g_k, (c) the mean fire size (MFS_j), and (d) the SD of fire size ($SDFS_j$) of each province. Each parameter was adjusted in 10% increments to ±50% of its baseline value (the asterisk on the x-axis represents the baseline value for each parameter, as defined in Table 1). Age classes follow those of Nonaka and Spies (2005), as listed in Table 3, but the two youngest classes were combined due to narrow class width and similarity in response to changes in input parameters. Beyond a 20% increase in g_k, the value of g_3 was held constant at 0.99.

effect on the proportion of the total area burned per year that is burned by fires in each size class (Q_k, Table 2), which influences the probability that a cell will be burned at high severity for each fire initiated in its province (Eq. (8)). However, it takes a very large change in the mean or SD of fire size to produce a substantial change in this value. For example, decreasing the mean fire size of the Coastal Province by 50% from its baseline value causes the expected proportion of the total area burned by large fires (>500 km^2) to decrease from its baseline value of 0.404 (Table 2) to 0.331. As a result, the area expected to burn at high severity each year within the 14,540-km^2 Coastal Province decreases by only 26 ha, with little effect on the expected abundance of each age class (Fig. 3c).

5. Discussion

5.1. New insight from the approximation

Analytical approximation of the computer simulation model, LADS (version 2.2; Wimberly, 2002), produces the abundance of seven age classes and two stand structures equivalent to that

Table 4
Equations used to calculate the expected proportion of the landscape covered by the semi-open and multi-story stand-structure classes, as defined by Wimberly (2002). Variables are defined in Table 2 and u is used as a dummy variable to clarify that the hazard rate for moderate-severity fire, $h_M^{(j)}(t)$ is a function of the limits of integration. The analytically determined abundance of each stand structure in the Coastal and Valley Margin provinces is provided in the third and fourth columns, respectively, with the abundance averaged over a 50,000-year simulation provided in parentheses.

Stand-structure class	Equation	Coastal Province	Valley Margin
Semi-open[a]			
AGE > 30 TFIRE ≤ 30	$\sum_{t=31}^{\infty}\left[a_{\infty}^{(j)}(t)\left\{1-\exp\left(-\int_{t-30}^{t}h_L^{(j)}(u)du\right)\right\}\right]$	6.0 (6.9)	16.4 (15.6)
Multi-story[a]			
AGE > 80 30 < TFIRE ≤ 80	$\sum_{t=31}^{\infty}\left[\begin{array}{c}a_{\infty}^{(j)}(t)\left\{1-\exp\left(-\int_{t-80}^{t-30}h_L^{(j)}(u)du\right)\right\}\\ \left\{\exp\left(-\int_{t-30}^{t}h_L^{(j)}(u)du\right)\right\}\end{array}\right]$	7.9 (8.9)	17.8 (16.3)

[a] AGE and TFIRE represent the time since the last high-severity fire and the time since the last fire of any severity, respectively, as used by Wimberly (2002) to define the semi-open and multi-open stand-structure classes.

averaged over time and across replications of the simulation model (Tables 3 and 4). The approximation provides a detailed understanding of the modeled fire regime without simulating a series of recurring fires or the forest response to each fire. It illustrates that in the Coastal Province, cells burn at high severity at a mean interval of 362 years and at low severity at a mean interval of 447 years (Table 2). Also, in the Coastal Province, only 2% of fires are of the large size class, where the proportion of fires in the kth size class is given by, $\Phi[\{\ln(Max_k) - \mu_j\}/\sigma_j] - \Phi[\{\ln(Min_k) - \mu_j\}/\sigma_j]$. However, this small percentage of fires that exceed 500 km^2 in extent accounts for 40% of the total area burned over a long simulation (Q_3; Table 2). In the Valley Margin, cells burn at high and low severity at mean intervals of 300 and 150 years, respectively (Table 2), where 96% of the fires are of the small size class ($\leq$100 km^2) and these fires account for account for 67% of the area burned over time (Q_1; Table 2).

Although LADS was parameterized to account for the spatial variation in the fire regime determined in an empirical fire-history study, none of the above values are provided in the simulation output to help validate the parameterization. The empirical study found evidence of at least two episodes of widespread, high-severity fire in the 16th century and another similar episode in the 19th century (Impara, 1997). Less extensive episodes with a mixed pattern of burn severity occurred more frequently than the high-severity episodes, but they were limited primarily to drier areas near the Willamette Valley.

The analytically determined values (Table 2) quantify how the differences in input parameters (Table 1) translate into different fire regimes between the two provinces. In particular, because fire size is modeled with a lognormal distribution and the probability of burning at high severity increases with fire size, relative differences in the frequency of low- and high-severity fire are determined by the parameters of the fire-size distribution. The mean and SD of fire size in the Coastal Province are large enough that for each ignition, the joint probability that a random cell is burned and fire severity is high ($P\{b_i = 1, \omega_i = 1\} = 2.77 \times 10^{-3}$; Eq. (8), Table 2) is greater than the joint probability that the cell is burned and fire severity is low ($P\{b_i = 1, \omega_i = 1\} = 2.25 \times 10^{-3}$). The latter probability was calculated following Eq. (8), but the proportion of burned cells expected to experience high-severity fire (g_k) was replaced with the proportion expected to burn at low severity ($1 - g_k$). Thus, the NFR for low-severity fire is longer than that for high-severity fire in the Coastal Province (Table 2), but the converse is true in the Valley Margin due to the smaller mean and SD of fire size.

After determining the hazard rates for high- and low-severity fire, it was possible to calculate the expected abundance of each age class (Eq. (9); Table 3). In addition, the limits of integration in Eqs. (10) and (11) can be adjusted to determine the expected abundance of any stand-structure type defined by the two state variables tracked for each cell in LADS (Table 4).

A primary benefit of the approximation is that it produces a series of equations that directly specify the roles of key input parameters (see Section 5.2). Also, the ability to calculate the expected abundance of each age class and stand-structure type without simulating a series of recurring fires or the spread and effects of each fire is highly valuable. The fire-spread algorithm of landscape-scale models of fire and forest dynamics usually is the most difficult algorithm to develop, the most time-consuming part of running the model, and it may be difficult to evaluate relative to empirical data.

5.2. Direct evaluation of parameter effects

The specification of the roles of key input parameters analytically differs from sensitivity analyses commonly applied to simulation models because equations directly illustrate the effect of the parameters rather than having to infer these effects indirectly from model output. Direct specification of parameter effects has the advantages that it can quickly be applied over a broad range of parameter values, it is not dependent on the number of model replications or simulation length, and it provides equations that aid in identifying scaling relationships among the parameters. For example, with all other input parameters fixed, the NFRs for low- and high-severity fire both scale linearly with the overall NFR of each province (Table 2).

The benefit of evaluating the effects of input parameters analytically is shown by the illustration of the reasons why changing parameters of the fire-size distribution has minimal effect on the expected abundance of each age class (Fig. 3c and d). Changing the mean or SD of fire size affects the expected age distribution only by changing the proportion of the total area burned that is expected to be burned by fires in each size class, Q_k, and its corresponding effect on the hazard rate for high-severity fire (Eq. (8), Table 2). However, these effects are minimal even after increasing or decreasing the mean or SD of fire size by as much as 50% from their baseline values (Fig. 3c and d).

Changing the mean or SD of fire size does affect the year-to-year variation in area burned, however, and this increased variance could be misinterpreted as an effect on the average abundance of each age class if it was evaluated using a sensitivity analysis with too few replications. For example, if mean fire size is increased, the expected number of fires per year (λ_j) decreases according to the relationship, $\lambda_j = A_j/(NFR_j \times MFS_j)$, in order to maintain the same mean annual area burned (A_j/NFR_j). However, with a larger mean fire size, this area will be burned by a smaller number of fires that are larger, on average, than under the baseline scenario. As a result, variation in annual area burned will increase relative to the baseline scenario, and it would take a longer model run or a larger number of replications to reach a stable mean abundance of each age class equivalent to that determined analytically.

5.3. Feedback of stand age on fire occurrence

LADS was designed with the intention that susceptibility of each cell to fire ignition and spread from adjacent cells follows a U-shaped function of stand age (Agee and Huff, 1987; Wimberly, 2002). Despite this intention, the age distributions produced analytically without accounting for the feedback of stand age on fire susceptibility was nearly identical to that produced by simulation (Table 3), which suggests this feedback has little or no influence on the average abundance of each age class over time. The reason for limited effect of this feedback lies primarily in the independence of the random variables that determine the area burned in each timestep from the forest conditions existing at that time. The number of fires per timestep in each province is modeled as a Poisson random variable, and the size of each fire is drawn from a lognormal distribution at the time of each ignition. Both random variables are independent of existing forest conditions.

The drawing of annual area burned independent of the existing forest conditions is consistent with a system where fire size is driven primarily by weather, and time since the previous fire has little or no feedback on fire occurrence (Bessie and Johnson, 1995). For example, a large number of fires could occur and large fire sizes could be drawn in a year when most of the landscape is in the least fire-prone age classes. Thus, fires could extinguish in the middle of a patch of highly susceptible vegetation or spread across a patch in the least susceptible condition depending on the fire size drawn at the time of ignition. The drawing of the number of fires per year and the size of each fire independent of existing landscape condition may be appropriate for the Oregon Coast Range, where some of the largest documented fires were driven by strong foehn winds that likely overrode variation in fuel loading associated with stand age

(Dague, 1934). However, this approach to determining annual area burned could be highly inaccurate in drier regions prone to more frequent fire, where spatial variation in fuel loading as a function of time since the previous fire is more likely to constrain fire extent (Collins et al., 2009).

Understanding how the independence of variables affecting annual area burned from existing forest conditions may override the feedback of stand age on fire susceptibility is essential before applying a model to regions with different relative strengths of weather and fuels in limiting fire extent (Meyn et al., 2007). Other widely used models, including LANDIS (He et al., 2005) and LANDSUM (Keane et al., 2006), also draw fire size from a known distribution at the time of ignition independent of the abundance of different forest conditions that year, which may weaken the feedback of time since fire on susceptibility to subsequent fire.

5.4. Exponential age distributions

Under a system where time since fire has no effect on the annual probability of fire occurrence (i.e., an age-independent hazard rate), the probability density functions for the fire-interval distribution and stand age both are exponential in form (Johnson and Gutsell, 1994). For the reasons stated in Section 5.3, the assumption that stand age has no feedback on the annual probability of fire occurrence appears reasonable for the Oregon Coast Range. Under this assumption, the hazard rate for high-severity fire in each province is the reciprocal of the NFR for high-severity fire: $h_{\tau}^{(j)} = 1/E^{(j)}(t)$ (Eq. (3)). Also, the density function for the intervals between successive high-severity fires for cells in each province $f_{\tau}^{(j)}(t)$ (Eq. (2)), is equivalent to the density function for stand age, $a_{\infty}^{(j)}(t)$ (Eq. (4)), in the respective province, and both are exponential in form. However, if time since fire more strongly affected the probability of a cell burning, the equilibrium age distribution would not be equivalent to the fire-interval distribution, and neither would be exponential (McCarthy et al., 2001).

Although the approximation of LADS produces an exponential age distribution for each province, the distribution of stand ages found in any year of the simulation fluctuates around this distribution (Wimberly et al., 2000). The degree of fluctuation is a function of the extent of the province relative to variation in annual area burned, as driven by variation in the number of fires per year and the size of each fire. Given the high SD of fire size (Table 1), the observed area burned per year fluctuates widely around the expected value, which allows the age distribution found in any year of the simulation to vary widely around $a_{\infty}(t)$. The degree of variation also increases when considering a subset of a province (Wimberly et al., 2000). However, if province area (A_j) was extended indefinitely, the average number of fires per year would increase according to the relationship, $\lambda_j = A_j/(NFR_j \times MFS_j)$ (Table 1). Thus, by the law of large numbers (Ross, 2002), with increasing numbers of fires per year, the mean size of the fires in any year of the simulation would approach MFS_j. Also, the area burned in any simulation year would approach the expected annual area burned, and the observed age distribution would approach the equilibrium age distribution. Averaging across a large number of replications would have a similar effect.

Despite an exponential form for the equilibrium age distribution of each province, the expected age distribution of the entire Coast Range is not exponential. Calculating the density function for stand age for a spatial mixture of fire regimes in the two provinces, each with different hazard rates for high-severity fire, requires first calculating the density function for stand age in each province, and then averaging these functions weighted by province area (Eq. (9)). This calculation is not equivalent to calculating an average hazard rate for the two provinces, and then using this hazard rate to determine the expected abundance of each age class (McCarthy and Cary, 2002). Similarly, under a temporally varying fire regime, where the expected area burned per year is not fixed, the probability density function for stand age in any year would not be exponential, even if the annual probability of fire was independent of stand age (Boychuk et al., 1997).

5.5. Limitations of the approximation

It is important to note that the approximation does not provide statistical distributions for the abundance of forest age classes or stand structures, and it provides no information on patch sizes or spatial patterns of the different forest structures. In addition, although the simplification of assuming that time since fire does not feedback on the annual probability of fire occurrence has little or no effect on the abundance of each age class and stand structure averaged over time and across simulation replicates, the approximation does not address whether the feedbacks of stand age incorporated into the fire-spread algorithm of LADS (Wimberly, 2002) lead to fine-scale spatial variation in the distribution of age classes and stand structures distinct from that produced under a scenario where stand age is not incorporated into the fire-spread algorithm.

Another aspect of LADS not addressed analytically is the effects of fire that spread across province boundaries. Because fire size is drawn at the time of ignition using fire-size parameters for the province where it is ignited, the spread of fires across province boundaries could lead to heterogeneity in the fire-size distribution for each province. Differences in the fire-size distribution between cells located near a province boundary and those further from the boundary are potentially important because the probability of a cell being burned at high severity is related to the size of the fire in which it burns. However, the effect of fires spreading across province boundaries on the expected age distribution of the Oregon Coast Range may be minor because each province is a single polygon and there is relatively little common boundary between them. If the landscape were a finer-scale mosaic of smaller zones with different fire-regime parameters, failure to account for the effects of fire spread among zones could lead to greater divergence between age distributions determined analytically and by simulation. However, in the case where most fires spread among zones, drawing fire size at the time of ignition based on parameters of the zone where the fire was initiated may poorly represent the fire-spread process.

6. Conclusions

Analytical approximation of the simulation model, LADS provides a detailed understanding of the modeled fire regime and clarifies the effects of key input parameters. Also, once the hazard rates for high- and low-severity fire are determined (Table 2), the expected abundance of each age class (Table 3) and different stand structures (Table 4) can be calculated directly, without generating a series of recurring fires. The development of an analytical approximation for LADS illustrates that analytical methods can account for much of the complexity more commonly addressed by simulation. In this case, they were applied to a system with (1) two provinces, each with a unique fire-interval and fire-size distribution, (2) variation in annual area burned driven by stochasticity in the number of fires per year and the size of each fire, (3) two fire severities that lead to two pathways of forest succession, and (4) greater representation of high-severity fire with increasing fire size.

Numerous other models use a series of random variables to determine the area burned each year and the size of each fire, and a rule-based approach associated with a state-and-transition succession model is used to model the effects of fire on forest

succession (Kurz et al., 2000; Keane et al., 2004; Scheller and Mladenoff, 2007; He, 2008). Thus, it is likely that methods similar to those developed in this study can be applied to gain greater understanding into the functioning of other landscape-scale forest simulation models.

For models that incorporate several spatially interactive processes (e.g., fire spread and seed dispersal) or employ more complex feedbacks of forest conditions on fire spread or severity, it may be difficult to approximate all of the model algorithms analytically. In these cases, comparing the simulation output to results of an analytical approximation that accounts for as much model behavior as possible provides a basis for interpreting the strengths and identifying thresholds in the processes that cannot be derived analytically (Ives et al., 1998).

As simulation models become increasingly complex and are increasingly applied to novel scenarios (e.g., changing fire regimes under a warming climate), it becomes increasingly important to better understand how these models work. Analytical approximation is not suggested as a substitute for simulation models, but rather, as a complementary approach aimed at providing greater insight into model function. Increasing the transparency of these models may clarify the degree of uncertainty in model output that can be attributed to input parameter values that were estimated. In addition, analytical approximation may help in identifying thresholds and scaling relationships among parameters, and determining whether the number of model replications is sufficient before evaluating output.

Acknowledgments

We thank Fred Swanson, Julia Jones, Tom Spies, Chris Daly, and two anonymous reviewers for feedback on the ideas presented in this paper and for reviews of an earlier draft. Mike Wimberly provided valuable feedback on an earlier draft and assisted with running LADS. Support for this research was provided by a National Science Foundation Integrative Graduate Education and Research Traineeship (IGERT) graduate fellowship in Ecosystem Informatics at Oregon State University (NSF Award 0333257), and by the H.J. Andrews Experimental Forest and Long-Term Ecological Research (LTER) Program (NSF DEB 0823380), the Pacific Northwest Research Station, and the James H. Duke, Jr. Graduate Fellowship, the Alfred W. Moltke Memorial Scholarship, and the College of Forestry Graduate Fellowship at Oregon State University.

References

Agee, J.K., Huff, M.H., 1987. Fuel succession in a western hemlock/Douglas-fir forest. Can. J. Forest Res. 17, 697–704.
Bessie, W.D., Johnson, E.A., 1995. The relative importance of fuels and weather on fire behavior in subalpine forests. Ecology 76, 747–762.
Boychuk, D., Perera, A.H., Ter-Mikaelian, M.T., Martell, D.L., Li, C., 1997. Modelling the effect of spatial scale and correlated fire disturbances on forest age distribution. Ecol. Model. 95, 145–164.
Collins, B.M., Miller, J.D., Thode, A.E., Kelly, M., van Wagtendonk, J.W., Stephens, S.L., 2009. Interactions among wildland fires in a long-established Sierra Nevada natural fire area. Ecosystems 12, 114–128.
Dague, C.I., 1934. The weather of the great Tillamook, Oreg., Fire of August 1933. Mon. Weather Rev. 62, 227–231.
DeAngelis, D.L., Mooij, W.M., 2003. In praise of mechanistically rich models. In: Canham, C.D., Cole, J.J., Laurenroth, W.K. (Eds.), Models in Ecosystem Science. Princeton University Press, Princeton, NJ, pp. 63–82.
He, H.S., 2008. Forest landscape models: definitions, characterization, and classification. Forest Ecol. Manage. 254, 484–498.
He, H., Li, W., Sturtevant, B.R., Yang, J., Shang, B.Z., Gustafson, E.J., Mladenoff, D.J., 2005. LANDIS 4.0 Users Guide. USDA For. Serv. Gen. Tech. Rep. NC-263, 93 pp.
Heinselman, M.L., 1973. Fire in the virgin forests of the Boundary Waters Canoe Area, Minnesota. Quaternary Res. 3, 329–382.
Impara, P.C., 1997. Spatial and temporal patterns of fire in the forests of the central Oregon Coast Range. Ph.D. Dissertation. Oregon State University, Corvallis.
Ives, A.R., Turner, M.G., Pearson, S.M., 1998. Local explanations of landscape patterns: can analytical approaches approximate simulation models of spatial processes? Ecosystems 1, 35–51.
Johnson, E.A., Gutsell, S.L., 1994. Fire frequency models, methods, and interpretations. Adv. Ecol. Res. 25, 239–287.
Keane, R.E., Parsons, R.A., Hessburg, P.F., 2002. Estimating historical range and variation of landscape patch dynamics: limitations of the simulation approach. Ecol. Model. 151, 29–49.
Keane, R.E., Cary, G.J., Davies, I.D., Falnnigan, M.D., Gardner, R.H., Lavorel, S., Lenihan, J.M., Li, C., Rupp, T.S., 2004. A classification of Landscape Fire Succession Models: spatial simulations of fire and vegetation dynamics. Ecol. Model. 179, 3–27.
Keane, R.E., Holsinger, L.M., Pratt, S.D., 2006. Simulating Historical Landscape Dynamics using the Landscape Fire Succession Model LANDSUM Version 4.0. USDA For. Serv. Gen. Tech Report RMRS-GTR-171CD, 73 pp.
Keane, R.E., Loehman, R.A., Holsinger, L.M., 2011. The Fire BGCv2 Landscape Fire and Succession Model: A Research Simulation Platform for Exploring Fire and Vegetation Dynamics. USDA For. Serv. Gen. Tech. Rep. RMRS-GTR-255, 137 pp.
Kurz, W.A., Bukema, S.J., Klenner, W.E., Greenough, J.A., Robinson, D.C.E., Sharpe, A.D., Webb, T.M., 2000. TELSA: the tool for exploratory landscape analysis. Comput. Electron. Agric. 27, 227–242.
Long, C.J., Whitlock, C., Bartlein, P.J., Millspaugh, S.H., 1998. A 9000-year fire history from the Oregon Coast Range, based on a high-resolution charcoal study. Can. J. Forest. Res. 28, 774–787.
McCarthy, M.A., Cary, G.J., 2002. Fire regimes in landscapes: models and realities. In: Bradstock, J., Williams, J., Gill, M. (Eds.), Flammable Australia: The Fire Regimes and Biodiversity of a Continent. Cambridge University Press, Cambridge, UK, pp. 77–94.
McCarthy, M.A., Gill, A.M., Bradstock, R.A., 2001. Theoretical fire-interval distributions. Int. J. Wildl. Fire 10, 73–77.
Meyn, A., White, P.S., Buhk, C., Jentsch, A., 2007. Environmental drivers of large, infrequent wildfires: the emerging conceptual model. Prog. Phys. Geogr. 31, 287–312.
Nonaka, E., Spies, T.A., 2005. Historical range of variability in landscape structure: a simulation study in Oregon, USA. Ecol. Appl. 15, 1727–1746.
Oreskes, N., 2003. The role of quantitative models in science. In: Canham, C.D., Cole, J.J., Lauenroth, W.K. (Eds.), Models in Ecosystem Science. Princeton University Press, Princeton, NJ, pp. 13–31.
Pielke Jr., R.A., 2003. The role of models in prediction for decision. In: Canham, C.D., Cole, J.J., Lauenroth, W.K. (Eds.), Models in Ecosystem Science. Princeton University Press, Princeton, NJ, pp. 111–138.
Reed, W.J., 1994. Estimating the probability of stand-replacing fire using the age-class distribution of undisturbed forest. Forest Sci. 40, 104–119.
Ross, S., 2002. A First Course in Probability, 6th ed. Prentice Hall, Upper Saddle River, NJ.
Scheller, R.M., Mladenoff, D.J., 2007. An ecological classification of Forest Landscape Simulation Models: tools and strategies for understanding broad-scale forested ecosystems. Landscape Ecol. 22, 491–505.
Teensma, P.D., Rienstra, J.T., Yoder, M.A., 1991. Preliminary Reconstruction and Analysis of Change in Forest Stand Age Class of the Oregon Coast Range from 1850 to 1940. U.S. Bureau of Land Management, Portland, OR, Tech. Note T/N OR-9.
Thompson, J.R., Johnson, K.N., Lenette, M., Spies, T.A., Bettinger, P., 2006. Historical disturbance regimes as a reference for forest policy in a multiowner province: a simulation experiment. Can. J. Forest Res. 36, 401–417.
Turner, M.G., Romme, W.H., 1994. Landscape dynamics in crown fire ecosystems. Landscape Ecol. 9, 59–77.
Wimberly, M.C., 2002. Spatial simulation of historical landscape patterns in coastal forests of the Pacific Northwest. Can. J. Forest Res. 32, 1316–1328.
Wimberly, M.C., Spies, T.A., Long, C.J., Whitlock, C., 2000. Simulating historical variability in the amount of old forests in the Oregon Coast Range. Conserv. Biol. 14, 167–180.